Extracellular Vesicle MicroRNAs From Corneal Stromal Stem Cell Enhance Stemness of Limbal Epithelial Stem Cells by Targeting the Notch Pathway

Leying Wang, Xizhan Xu, Qiankun Chen, Yuan Wei, Zhenyu Wei, Zi-Bing Jin, and Qingfeng Liang

Beijing Institute of Ophthalmology, Beijing Tongren Eye Center, Beijing Tongren Hospital, Capital Medical University, Beijing, China

Correspondence: Qingfeng Liang, Beijing Institute of Ophthalmology, Beijing Tongren Eye Center, Beijing Tongren Hospital, Capital Medical University, Beijing 100005, China; lqflucky@163.com.

Received: April 10, 2023
Accepted: September 7, 2023
Published: September 28, 2023

Citation: Wang L, Xu X, Chen Q, et al. Extracellular vesicle microRNAs from corneal stromal stem cell enhance stemness of limbal epithelial stem cells by targeting the notch pathway. *Invest Ophthalmol Vis Sci.* 2023;64(12):42. https://doi.org/10.1167/iovs.64.12.42

Purpose. The limbal niche supports the self-renewal of limbal epithelial stem cells (LESCs). The corneal stromal stem cell (CSSC) is an important component in the niche that regulates the LESC phenotype. However, the intercellular communication between LESCs and CSSCs has yet to be elucidated.

Methods. A traditional two-dimensional (2D) system, a direct three-dimensional (3D) system, and an indirect 3D coculture system of LESCs and CSSCs were used to elucidate the paracrine pathway effect of CSSCs on LESCs. To reveal the impact of CSSC derived extracellular vesicles (CSSC-EVs) on LESCs, GW4869 and CSSC-EVs were added separately to the LESC culture medium. The outgrowth rate, cell density, differentiation, and stemness maintenance were compared among these methods. The miRNAs in the CSSC-EVs were sequenced, and the targeted Notch pathway was further confirmed by RT–qPCR and Western blotting.

Results. Compared with 2D culture, both the direct and indirect 3D coculture systems yielded a higher outgrowth rate and expression of stem cell markers of LESCs. The phenotypes of LESCs cultivated using the two coculture approaches were also comparable. Nevertheless, GW4869 inhibited the effect of CSSCs on LESCs, and the addition of CSSC-EVs to the 2D culture system could increase cell density, and the proportion of $p63\alpha^{bright}$ cells, which indicated that CSSC-EVs were crucial in regulating LESCs. Furthermore, the EV-AlixKD with reduced miRNA partly lost its regulating function. The abundant miRNAs in CSSC-EVs, such as hsa-miR-663b, hsa-miR-16-5p, and hsa-miR-1290, target the Notch pathway. The LESCs transfected with miR-663b had higher p63 expression via downregulating of the Notch pathway.

Conclusions. CSSC-EV played an important role in promoting LESC proliferation and stemness maintenance by targeting Notch signaling via miRNAs, which will increase our understanding of the limbal niche and provide a potential new approach for LESC culture and the treatment of corneal epithelial disorders.

Keywords: limbal epithelial stem cell (LESC), corneal stromal stem cell (CSSC), extracellular vesicle (EV), Notch pathway

Limbal epithelial stem cells (LESCs) located in the niche of the basal layer of the limbus are adult stem cells with self-renewal potential.[1] As seed cells, LESCs are essential for maintaining the integrity of the corneal epithelium and normal visual function. Damage to the LESCs and their niche by chemical burns, long-term contact lens wearing, chronic inflammation, etc., could lead to limbal stem cell deficiency (LSCD).[2] In such circumstances, the cornea is invaded by conjunctival epithelial cells and accompanied by ocular irritation symptoms, impaired vision, persistent epithelial defects, and neovascularization.[3] Furthermore, functional LESCs are fundamental for successful keratoplasty. Failing to address LSCDs may raise the failure rate of keratoplasty and the risk of immunologic rejection for subsequent keratoplasty.[4]

Limbal stem cell transplantation is the common treatment for LSCD. Transplantation of in vitro-expanded LESCs is becoming a promising technique compared to traditional direct limbal transplantation because it requires a small biopsy, especially in bilateral LSCD cases.[5] However, the standard protocol to cultivate LESCs using mouse 3T3 fibroblasts as feeder cells may result in surrogate niche cells secreting the necessary factors but containing animal ingredients. Moreover, the overall success rates of cultivated limbal epithelial transplantation procedures were reported to range from 50 to 85%,[6] and long-term regeneration of the corneal surface often failed to be satisfactory due to recurrent corneal neovascularization, which was speculated to be caused by an abnormal limbal microenvironment.[7] Currently, most studies of in vitro LESCs concentrated on

the regulatory functions of chemical molecules, but there is still a long way to go before clinical applications. Exploring the crosstalk between LESCs and limbal niche cells might provide new perspectives in elucidating the molecular regulation of LESCs by niche factors, modifying the culture system that potentially simulates the limbal microenvironment to improve the prognosis after limbal epithelial transplantation.

Corneal stromal stem cells (CSSCs) are important niche cells that demonstrate similar properties to mesenchymal stromal cells.[8] Mounting evidence has verified that the interactions between LESCs and mesenchymal stromal cells are essential for preserving the stemness of LESCs.[9,10] Nevertheless, the potential mechanism of communication between CSSCs and LESCs has not been elucidated in detail. It was assumed that CSSCs exerted their effect on LESCs mostly through a paracrine mechanism rather than direct cell contact considering that most of the CSSCs were retained in the anterior corneal stroma.[11] Extracellular vesicles (EVs), as an important part of paracrine fashion, have attracted extensive attention and can transfer bioactive molecules among cells and regulate the phenotype of targeted cells.[12] Besides, EVs are a noncell product that is safe with low immunogenicity,[13] and easy to process into medium supplement and topical eye drops, which set the foundation for its application.

In this study, we investigated the paracrine function of CSSCs in regulating LESCs with a 3D coculture system and were specifically interested in determining whether CSSC-EVs were crucial in affecting LESCs by transferring miRNAs and modulating Notch signaling. These findings would help in understanding the niche of LESCs and provide a bright and safe strategy for LESCs culture and LSCD administration.

Materials and Methods

Human Tissues and Study Approval

Human sclerocorneal tissues were obtained from the Beijing Tongren Eye Bank (Beijing, China) with the approval of the Institutional Review Board (TRBCK12019-129) and processed in accordance with the tenets of the Declaration of Helsinki. The death-to-preservation time and death-to-experiment time were less than 12 hours and 10 days, respectively. Optisol was used to submerge the tissue up until the experiment.

Corneal Stromal Stem Cell Culture

For the culture of CSSCs, the human limbal ring, measuring 3 mm in width, was isolated. Subsequently, the corneal epithelium and iris were mechanically removed, and the posterior stroma, endothelium, and tenons were meticulously excised using surgical scissors. The remaining rim was then divided into 12 segments, with each tissue piece being placed in 12-well plate. The ingredients of the CSSC culture medium were as follows: MEMA Alpha basic, 10% (v/v%) fetal bovine serum, 1 × penicillin/streptomycin, and 1 × nonessential amino acids. Cells were grown at 37°C in an atmosphere of 5% CO_2 for approximately 14 days, and the medium was changed every 2 to 3 days. CSSCs at passages 3 to 5 were used for the following study.

Limbal Epithelial Stem Cell Culture

LESCs were cultured under three different culture methods: a 2-dimensional (2D) method, the direct 3-dimensional (3D) method, and the indirect 3D method (Fig. 1A). A 4.67 cm^2 polyester membrane with a 0.4 µm pore size was chosen in the culture system. The standard culture medium of LESCs for the 3 culture systems was described as follows: DMEM and DMEM/F12 (1:1) with 10% fetal bovine serum, 10 ng/mL epidermal growth factor, 5 µg/mL insulin, 10^{-10} M cholera toxin, 0.4 µg/mL hydrocortisone, and 2×10^{-9} M 3,3,5-triiodo-L-thyronine.[14]

The limbal explant with an intact epithelial layer was plated on the inner side of the polyester membrane in the 2D method's center without the assistance of CSSCs. For the 3D coculture method, the CSSCs were pretreated with 30 µg/mL mitomycin C for 2 hours when the confluence reached 70% to 80%. In the direct 3D method, the pretreated CSSCs were seeded on the opposite sides of a polyester membrane (density of 2000 cells/cm^2) for 2 hours to allow the cells to attach to the membrane.[9] In the indirect 3D method, CSSCs were seeded on the bottom of a 6-well plate at a density of 2000 cells/cm^2. Then, the insert was placed upright, and the limbal explant was placed in the center of the polyester membrane, as described in the 2D method.

Extracellular Vesicles Collection and Identification

EVs were purified and collected from the supernatant of CSSC that was cultured using EV-free fetal bovine serum (EXO-FBS-50A-1, SBI) for 48 hours by sequential ultracentrifugation. For elimination of cell debris, the medium was centrifuged at 2000 × *g* for 10 minutes at 4°C. The supernatant was collected and spun at 10,000 × *g* for 30 minutes and 100,000 × *g* for 70 minutes twice. The precipitate containing EVs was resuspended in phosphate-buffered saline (PBS) and stored at −80°C for the following study. The morphology of the EVs was examined using transmission electron microscopy (TEM; JEM-2100, Japan). The particle size distribution was measured with a NanoSight system (NanoSight, Amesbury, UK). The protein expression of Alix, TSG101, and CD81, was detected by Western blotting. The EVs was then added to the LESC medium at a final concentration of 1.65×10^6 particles/mL, 3.3×10^6 particles/mL, and 6.6×10^6 particles/mL at days 1, 3, and 5, which mimics the in vivo condition where LESCs would be continually exposes to CSSC-EVs.

Exosome Labeling

The isolated EVs were mixed with PKH67 (UR52303; Umibio, China), vortexed for 1 minute and incubated for 10 minutes at room temperature. The mixture of EVs and PKH67 was added to 10 mL of PBS and then enriched by centrifugation as mentioned above to obtain labeled EVs. Next, the labeled EVs were incubated with LESCs in medium at 37 °C for 4 hours. After the nuclei were stained with 4′,6-diamidine-2-phenylindole dihydrochloride (DAPI; C1006; Beyotime, China), the staining was observed with a fluorescence microscope (CX53; Olympus, Japan).

Exosome Inhibition Assay

For analysis of the role of CSSC-EVs in supporting the growth and stemness maintenance of LESCs, GW4869, an inhibitor

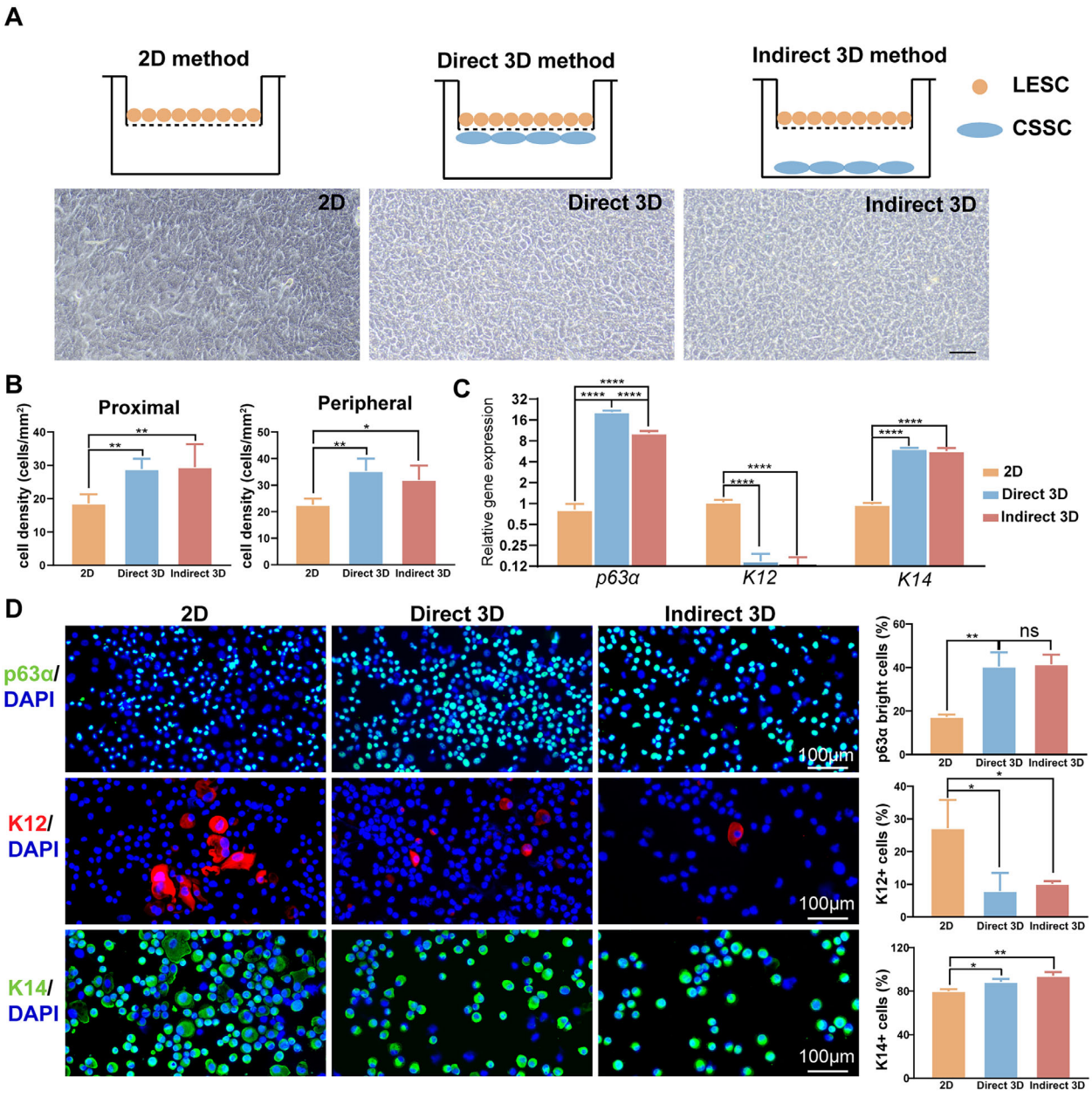

Figure 1. CSSCs mediated the LESC phenotype in both direct and indirect ways. (**A**) Schematic representation of different culture systems: 2D method, direct 3D method, and indirect 3D method. Morphology and outgrowth rate of LESCs in different culture systems (scale bar = 50 μm). (**B**) The cell density of LESCs with the direct 3D and indirect 3D methods was significantly higher than that with the 2D method. The quantitative results of PCR (**C**) and immunofluorescence staining (**D**) showed that the expression levels of p63α and K14 were increased, accompanied by decreased expression of K12, with the direct 3D method and indirect 3D method compared with the 2D method.

of EV generation, was added to the plate well. The optimal concentration of GW4869 was comprehensively determined by the cell toxicity and efficiency of inhibition of EV secretion. Cell toxicity was detected by the CCK8 kit. The efficiency of GW4869 was measured by collecting EVs from a 20 mL culture medium and then using a CD81 ELISA kit. When comparing the efficiency of the GW4869 method and the indirect 3D method in cultivating LESCs, we added an equal volume of a GW4869 solvent, dimethyl sulfoxide (DMSO), to the indirect 3D system.

siRNA Knockdown of Alix Expression

CSSCs cultured overnight in T75 culture flask were transfected with 50 nM Alix siRNA or a scrambled control siRNA using Lipo6000 transfection reagent (Beyotime Biotechnology, China) for 6 hours. Then, CSSCs were culture for 48 hours in EV-free CSSC medium. The real-time PCR and Western blotting of CSSCs were conducted to confirm the knockdown efficiency. The EVs were prepared as mentioned above.

The Growth and Morphology of LESCs

The expanded LESCs were monitored, and the cell morphologies were evaluated under a microscope (CX53; Olympus, Japan). When confluence was reached, the density of LESCs in the area proximal and peripheral to the explant was calculated as the average of the quantitative analysis results from four quadrants.

Quantitative Real-Time PCR

Total RNA was extracted from cultured LESCs with an RNAprep pure cell kit (DP430; Tiangen, China). The cDNAs were generated by reverse transcription of the total RNA with a HiScript III All-in-one RT SuperMix Kit (R333; Vazyme, China) according to the manufacturer's protocol. Quantitative PCR was performed with Taq Pro Universal SYBR qPCR Master Mix (Q712; Vazyme, China). Relative changes in gene expression were calculated using the 2-ΔΔCT method normalized to the GAPDH gene. The primers are listed in Supplementary Table S1.

Immunocytochemistry

Cytospin slides from cultured LESCs were prepared by a cytocentrifuge and subsequently stored at −20°C. Fixation was performed with 4% paraformaldehyde at room temperature for 15 minutes. Nonspecific binding sites were blocked, and the cells were permeabilized by 1% bovine serum albumin and 0.5% Triton X-100 for 30 minutes at room temperature. Cells were incubated with primary antibodies against p63α (ab124762), keratin 12 (K12, sc-515882), and keratin 14 (K14, ab7800). Incubation with secondary antibodies was performed at room temperature for 1 hour. Nuclei were labeled with DAPI for 10 minutes. Images were acquired by fluorescence microscopy. The percentages of p63α^{bright} cells, K12-positive cells, and K14-positive cells were counted by ImageJ (distributed by the National Institutes of Health).

Western Blotting

Equal amounts of protein were electrophoresed on 10% PAGE gels and transferred to a polyvinylidene fluoride membrane with the wet transfer system. The membranes were blocked with 5% skim milk for 1 hour and incubated at 4°C overnight with the primary antibody. For EV identification, primary antibodies included anti-TSG101 (ab125011; Abcam), anti-CD81 antibody (ab109201; Abcam), and Alix antibody (12422-1-AP; Protein Tech). For detection of the expression of the Notch pathway, the following primary antibodies were used: Notch1 (ab52627; Abcam), NICD (D3B8; Cell Signaling), Hes1 (ab108937; Abcam), and GAPDH (1E6D9; Protein Tech).

Small RNA Sequencing and Bioinformatic Analysis

Unique molecular indices (UMIs) were used to minimize errors. The QIAseq miRNA Library Kit for Illumina was used to create short RNA libraries for sequencing. Cutadapt (version 2.7) and Perl5 (version 26) software were used to remove reads with low quality that were smaller than 12 bp and to identify UMIs. The mapping of the UMIs to miRbase was performed using Bowtie (version 1.2.2).

miRNA Isolation and Analysis

Small RNAs from CSSCs or purified EVs were isolated using the MiPure cell/tissue miRNA kit (RC201; Vazyme, China) and were reverse transcribed using the miRNA first strand cDNA Synthesis kit (MR101; Vazyme, China) using a stem-loop approach. The miRNA quantification was conducted using miRNA universal SYBR qPCR master mix (MQ101; Vazyme, China), with U6 serving as the reference gene.

Statistical Analysis

The results of the current study were obtained from at least three repeat experiments. Statistical analysis was calculated by Prism version 8.0 software (GraphPad Software, Inc., San Diego, CA, USA). All quantitative data are presented as the means ± standard deviations. For statistical comparison, either a two-tailed unpaired Student's *t*-test (for 2 groups) or a 1-way ANOVA with post hoc Tukey's test (for more than 2 groups) was used. The threshold for statistical significance was set at $P < 0.05$.

Results

CSSCs Promote the Proliferation and Maintain the Stemness of LESCs Via a Paracrine Mechanism

The identification of MSCs were evaluated by morphology and mesenchymal stromal cell markers and multipotential differentiation (Supplementary Fig. S1). LESCs cultured using the 2D method displayed a more differentiated morphology than those cultivated using the direct 3D method and indirect 3D method that with very compact and uniform outgrowths containing small and cuboidal LESCs (see Fig. 1A). Moreover, the cell density of the proximal area and peripheral area of limbal biopsy outgrowth was significantly increased in the 2 coculture systems compared with the 2D system (all $P < 0.05$; Fig. 1B).

The mRNA expression of the classic putative LESC markers p63α and K14 and the differentiated corneal epithelial cell marker K12 was measured (Fig. 1C). LESCs cultured with the direct 3D method showed the highest expression of p63α, followed by the indirect 3D method and then the 2D method. A lower K12 mRNA level was detected in LESCs cultured with the direct 3D method ($P = 0.010$) and indirect 3D method ($P = 0.019$) than in those cultured with the 2D method. K14 mRNA expression was increased in LESCs grown utilizing the 2 coculture systems compared to the 2D method (both $P < 0.001$). At the protein level, the population of LESCs that expressed p63α, K12, and K14 stained by immunofluorescence was quantified (Fig. 1D). A significant increase in the percentage of p63α^{bright} cells was found with the direct 3D (40.5%, $P = 0.043$) and indirect 3D methods (41.5%, $P = 0.030$) compared with the 2D method. Moreover, both 3D methods were able to generate a similar percentage of p63α^{bright} cells ($P = 0.999$). K12 and K14 protein expression levels were consistent with their mRNA results. In general, the coculture system appeared to retain undifferentiated LESCs. Moreover, the direct 3D method and indirect 3D method exhibited similar effects in regulating the phenotype of LESCs, suggesting that paracrine signaling might play an important role in CSSC-LESC communication.

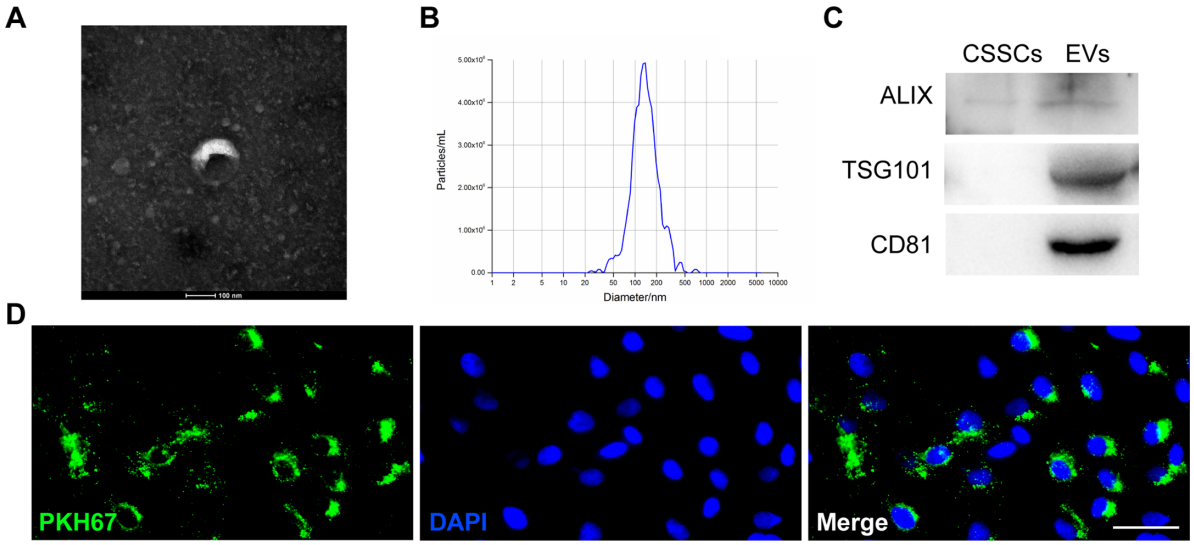

Figure 2. Identification and uptake of extracellular vesicles. (**A**) Representative images of CSSC-EVs by transmission electron microscopy showed the characteristic cup-shaped morphology. (**B**) The average diameter of extracellular vesicles was 130.7 nm. (**C**) Western blot analysis showed positive expression of Alix, TSG101, and CD81 in EVs and negative expression in CSSCs. (**D**) Uptake of CSSC-EVs by LESCs in vitro (scale bar = 50 µm).

The EVs Secreted by CSSCs can be Taken up by LESCs

EVs, as a communicator between cells, were isolated from CSSC-conditioned medium using the ultracentrifugation method and identified by morphology, size distribution, and biomarkers. Under TEM, the CSSC-EVs exhibited the characteristic cup-like structure (Fig. 2A). The average size of CSSC-EVs was 130.7 nm (Fig. 2B). Western blot analysis demonstrated that the EVs expressed specific markers, such as Alix, TSG101, and CD81, which were negative or expressed at low levels in CSSCs (Fig. 2C; Supplementary Fig. S3). To verify that CSSC-EVs can be taken up by LESCs, we prestained the CSSC-EVs with PKH67 and added them to LESCs in a 2D culture system. The images showed that the nuclei were surrounded by dotted green fluorescence, which ensured that the CSSC-EVs were endocytosed by LESCs (Fig. 2D).

Inhibition of EVs Secretion of CSSCs Weakens Their Ability to Promote LESCs

To determine whether CSSC-EVs affected LESCs, we used GW4869, an EV secretion inhibitor. The CCK8 results showed that 5 µM and 10 µM GW4869 had no obvious effect on the morphology and proliferation of CSSCs, whereas 15 µM and 20 µM GW4869 exhibited significant cell toxicity. Moreover, the quantitative results demonstrated that when the concentration of GW4869 reached 10 µM, the secretory exosome protein level dropped by approximately 40% (Supplementary Fig. S2). Thus, 10 µM GW4869 was applied in the following experiment.

GW4869 or its solvent DMSO was added to the well plate, as shown in Figure 3A, and denoted as the 3D-Ctrl or 3D-GW4869 method. The morphology of LESCs was smaller and more regular with the 3D-Ctrl than with the 3D-GW4869 method. The density of LESCs in the proximal area of biopsy was significantly higher with the 3D-Ctrl method than with the 3D-GW4869 method ($P < 0.001$; Fig. 3B). In addition, the 3D-Ctrl method yielded a higher expression of p63α and a lower expression of K12 than the 3D-GW4869 method ($P = 0.003$ and $P = 0.009$). Although K14 gene expression was lower with the 3D-Ctrl than with the 3D-GW4869 method, statistical significance was not shown ($P = 0.100$; Fig. 3C). Immunofluorescence further confirmed the higher expression of p63α and K14 and the lower expression of K12 ($P = 0.01$, $P = 0.001$, and $P = 0.006$; Fig. 3D). Collectively, the CSSC-EVs appeared to contribute to maintaining undifferentiated LESCs.

CSSC-EVs Promote the Stem Cell Characteristics of LESCs

To investigate the effect of CSSC-EVs on LESCs, we added CSSC-EVs to the medium of LESCs cultured by the 2D method. The morphology of CSSC-EVs was more regular in CSSC-EV-treated LESCs, as shown in Figure 4A. Compared to that of the 2D-Ctrl group with no culture of CSSC-EVs, the density of LESCs in the limbal biopsy periphery was considerably higher in the 1.65×10^6 particles/mL and 3.3×10^6 particles/mL CSSC-EV groups (24.5 ± 4.0 vs. 35.4 ± 7.4 cells/mm^2, $P = 0.003$; 24.5 ± 4.0 vs. 37.4 ± 7.4 cells/mm^2, $P < 0.001$; Fig. 4B). The p63α and K14 gene expression levels were significantly higher in the 3.3×10^6 particles/mL CSSC-EV-treated LESCs than in the 2D-Ctrl group (both $P < 0.001$; Fig. 4C). Immunostaining for p63α^{bright} cells was detected in $72.8 \pm 8.2\%$ of the cultured cells in the 3.3×10^6 particles/mL CSSC-EV-treated group, which was significantly higher than that in the control group ($47.2 \pm 11.1\%$, $P = 0.009$). In addition, the staining of the differentiation marker K12 was significantly decreased in the 3.3×10^6 particles/mL CSSC-EV-treated LESCs compared with the control cells ($18.5 \pm 2.0\%$ vs. $43.1 \pm 7.2\%$, $P = 0.008$). The percentage of K14+ cells was not significantly different among all groups (Figs. 4D, 4E). Generally, 3.3×10^6 particles/ml CSSC-EVs were the most effective for maintaining the stemness phenotype and were used for the following study.

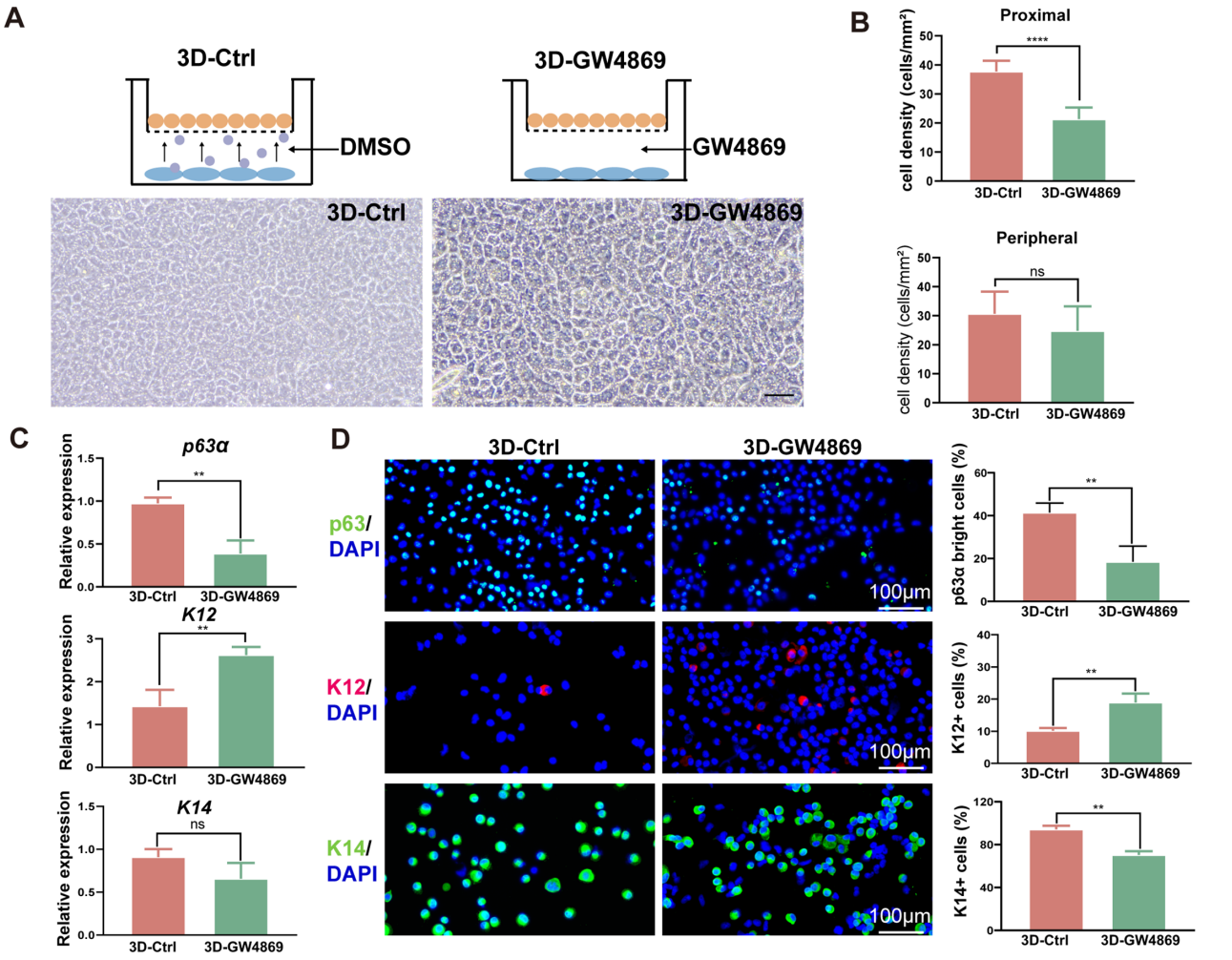

Figure 3. Inhibition of CSSC-EVs weakens CSSC-mediated LESC stemness maintenance. (**A**) Schematic representation of the indirect 3D method and GW4969 method. Morphology of LESCs in the 3D-Ctrl method and 3D-GW4869 culture system (scale bar = 50 μm). (**B**) The cell density of LESCs on the central and peripheral of the transwell were both higher with the indirect 3D method and GW4869 method. Quantitative real-time PCR (**C**), immunofluorescence staining and quantification of p63α^{bright} cells, K12+ cells and K14+ cells (**D**) showed that the GW4869 method increased K12 expression and suppressed p63α and K14 expression compared to the indirect 3D method.

miRNAs Are Candidate Effectors of CSSC-EVs Mediating the LESC Phenotype

To identify the potent miRNAs that contributed to the CSSC-EV-mediated phenotype of LESCs, we performed small RNA sequencing. The UMIs of the top 10 most abundant miRNAs are listed in Figure 5A and accounted for 44% of the total miRNA in the CSSC-EVs, of which hsa-miR-663b was the most prevalent miRNA (6%; Fig. 5B).

The role of EV miRNA in regulating LESCs was detected by generating EVs with CSSC-AlixKD. Downregulation of Alix protein affected the miRNA packaging in EVs. The results showed the Alix expression of CSSC was significantly reduced by siRNA transfection (Fig. 5C; Supplementary Fig. S3). The levels of the two most abundant miRNAs in EV-Ctrl were effectively reduced in EV-AlixKD (Fig. 5D).

When comparing the LESCs phenotypes with 2D-Ctrl, the density of LESCs in the limbal biopsy periphery was significantly increased in EV-Ctrl groups and then followed by EV-AlixKD (Fig. 5E). The qPCR analysis demonstrated the K14 gene expression were increased in both EV-Ctrl and EV-AlixKD groups. Moreover, p63α gene expression levels were significantly higher in EV-Ctrl group than 2D-Ctrl and EV-AlixKD groups (Fig. 5F). The immunofluorescent staining also showed the highest percentage of p63α^{bright} cells in EV-Ctrl group (Fig. 5G). In general, Alix knockdown reduced the ability of EVs in mediating the LESC phenotype.

miR-663b Regulated LESC Phenotype by Targeting the Notch1 Pathway

The Notch signaling pathway plays an important role in regulating stem cell self-renewal in adult organ systems. Thus, the Notch signaling pathway-associated targets of the top 10 miRNAs were predicted using TargetScan version 8.0. As shown in Figure 6A, Notch1 and Cyclin D1 were targeted by hsa-miR-663b, hsa-miR-16-5p, and hsa-miR-1290, which suggested that inhibiting the Notch pathway might be a potent mechanism by which CSSC-EVs regulate the LESC phenotype. LESCs cultured in 2D with or without miR-663b transfection were compared to verify this hypothesis.

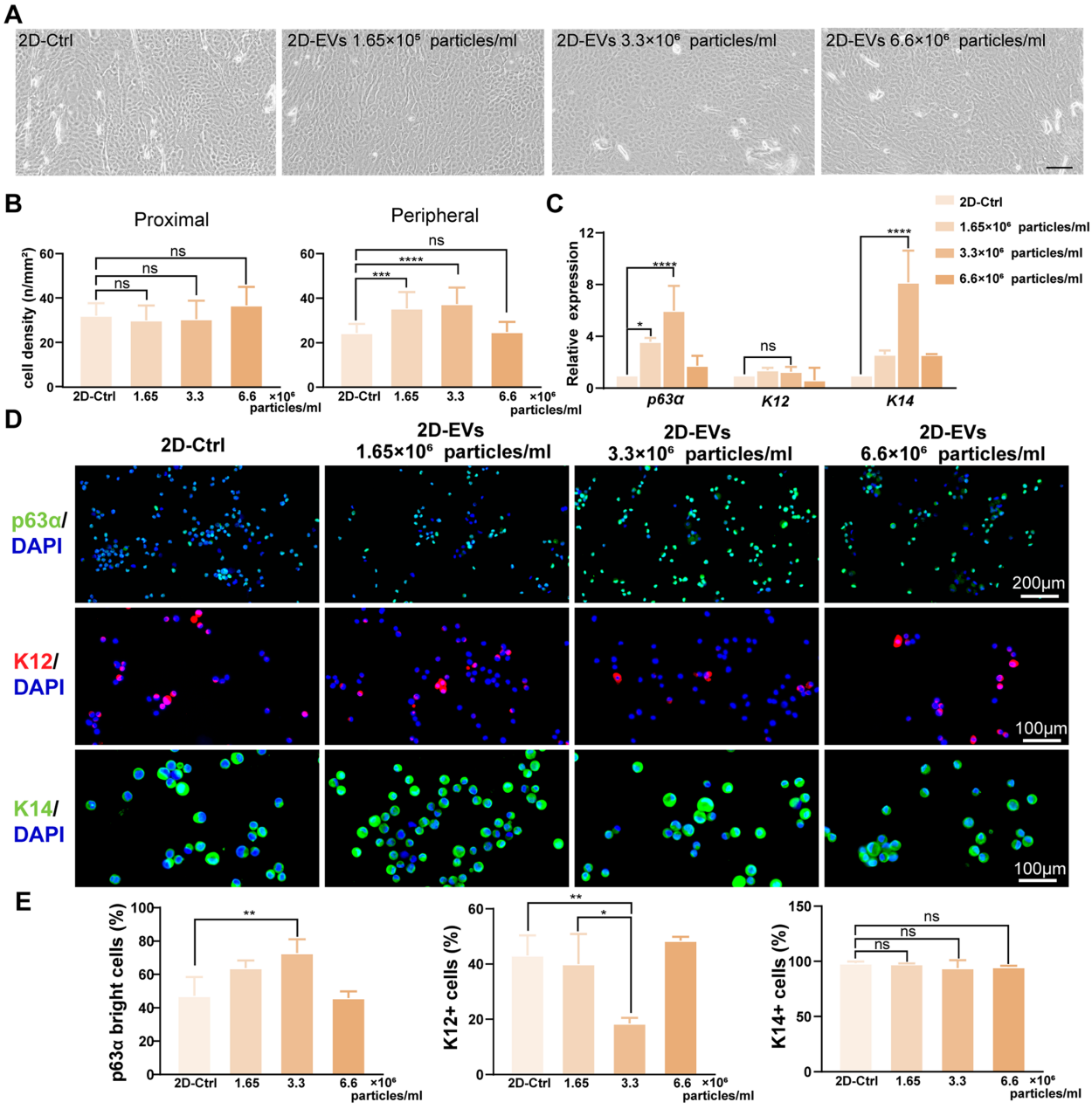

Figure 4. CSSC-EVs maintain the stemness of LESCs. (**A**) Morphology of LESCs cultured at different concentrations of CSSC-EVs. (**B**) The quantitative results showed that the cell density of LESCs in the proximal area was similar among the four different CSSC-EV concentrations. However, the peripheral cell density was significantly higher in the 3.3 × 10^6 particles/ml CSSC-EV-treated group than in the other groups. (**C**) The relative gene expression of p63*α* and K14 was significantly increased in the 3.3 × 10^6 particles/mL CSSC-EV-treated group. (**D**) Representative immunofluorescence images of p63*α*, K12, and K14 in LESCs treated with different concentrations of CSSC-EVs are shown. (**E**) The number of p63α^{bright} cells was significantly increased, and the number of K12+ cells was decreased in the 3.3 × 10^6 particles/mL CSSC-EV-treated group. The percentage of K14+ cells was similar among the different CSSC-EV concentration groups.

The PCR confirmed the successful transfection of miR-663b in LESCs (Fig. 6B). The p63*α* expression was significantly increased and the K12 gene expression was lower in miR-663b treated LESCs than 2D-Ctrl (see Fig. 6B). Immunofluorescence further confirmed the higher expression of p63*α* and the lower expression of K12 (Fig. 6C). Additionally, the PCR results showed that *Notch1* and *Hes1* were significantly downregulated in the miR-663b-treated LESCs compared to those of the 2D culture method. Similar to the gene expression results, the protein levels of Notch1, NICD, and Hes1 were also significantly decreased in CSSC-EV-treated LESCs compared with 2D-Ctrl method (Fig. 6D; Supplementary Fig. S3). Thus, the miR-663b, the most abundant miRNA carried by CSSC-EVs, promoted stemness of LESCs by inhibiting the Notch1 pathway.

Based on these findings, CSSC-EVs are essential for cell-cell communication between CSSCs and LESCs and for regulating the proliferation, stemness maintenance, and differentiation of LESCs, which is partially mediated by miRNAs enriched in CSSC-EVs, especially miR663b, that target the Notch1 signaling pathway in LESCs. A schematic illustration is presented in Figure 7.

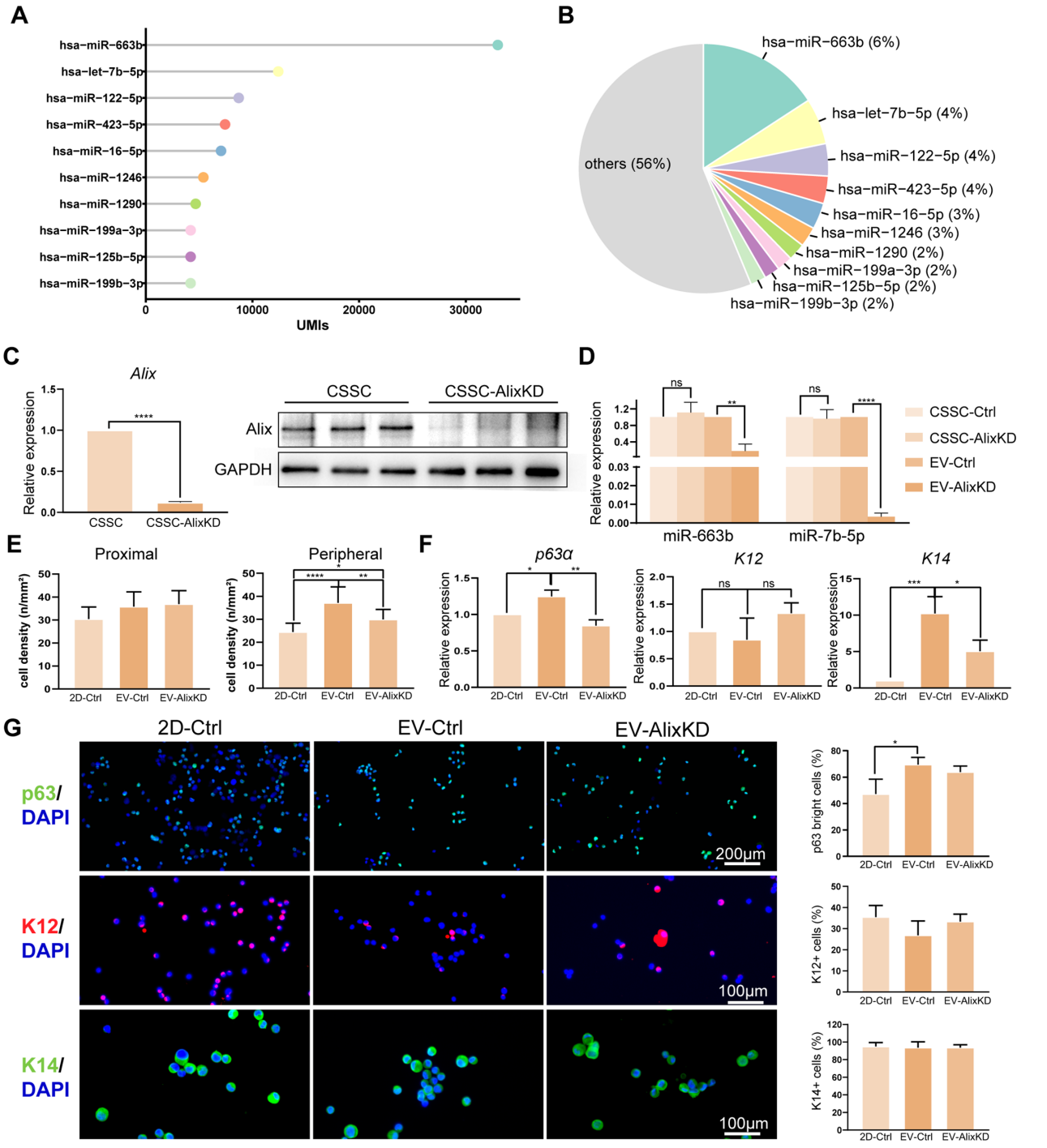

Figure 5. The miRNAs in CSSC-EVs regulate the phenotype of LESCs. (**A**) The lollipop chart shows the UMIs of the top 10 most abundant miRNAs in CSSC-EVs. (**B**) The top 10 most abundant miRNAs contributed 44% of the total miRNAs in CSSC-EVs. (**C**) The PCR and WB results showed that Alix expression was significantly lower in CSSC-AlixKD cells compared to untreated CSSCs. (**D**) The most abundant miRNAs in EVs-Ctrl were significantly decreased in EVs-AlixKD. (**E**) The quantitative results showed that the cell density of LESCs in the proximal area was similar among the untreated, EVs-Ctrl, and EVs-AlixKD groups. However, the peripheral cell density was significantly higher in the EVs-Ctrl group than in the other two groups. (**F**) The relative gene expression of p63α and K14 was significantly increased in the EVs-Ctrl group. (**G**) The number of $p63\alpha^{bright}$ cells was significantly increased in EVs-Ctrl group. The percentage of K12+ cells and K14+ cells had not statistically difference among the three groups.

Investigative Ophthalmology & Visual Science

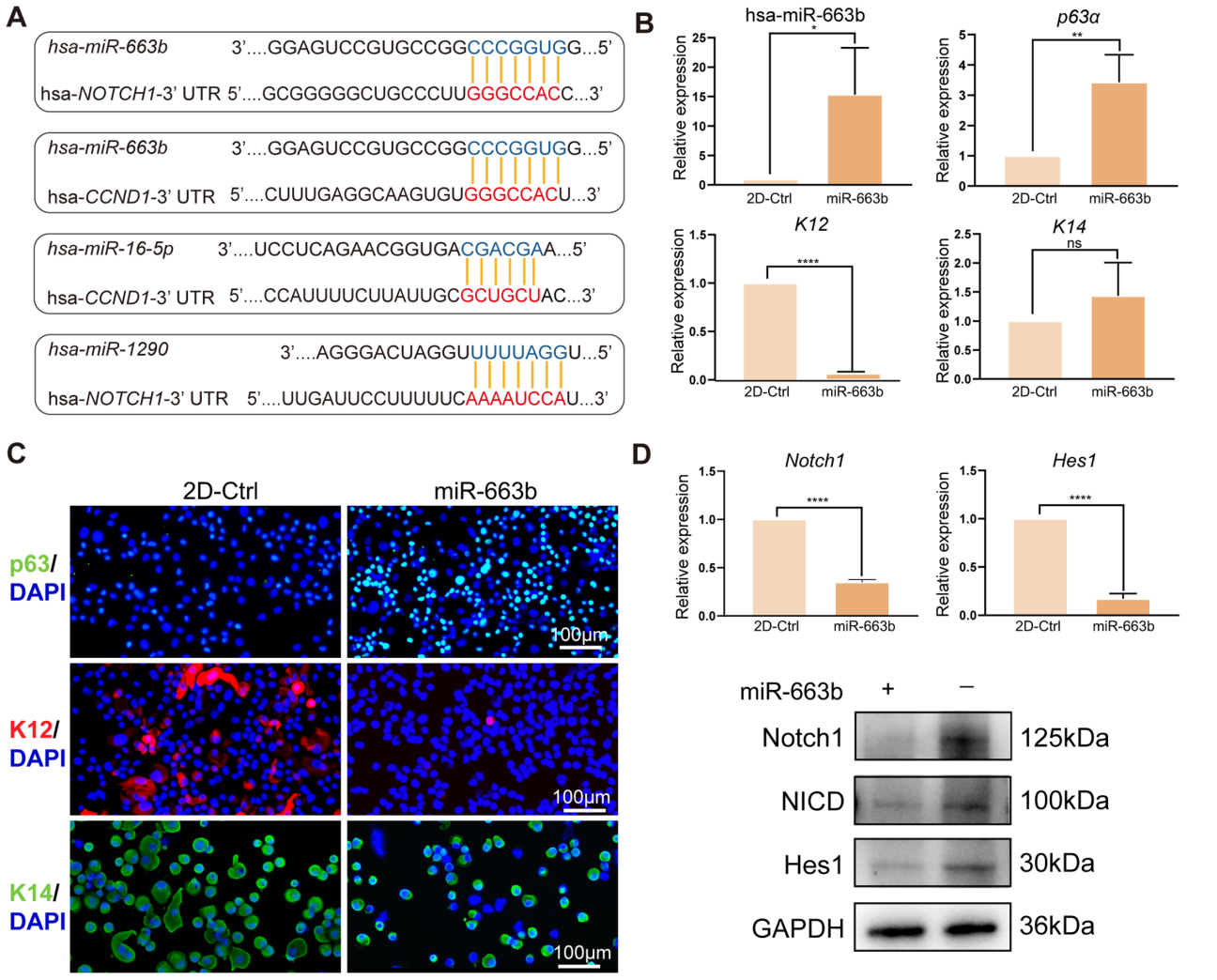

Figure 6. The miR-663b was the candidate mediator of CSSC-EVs for managing LESCs phenotype. (**A**) Predicted target sites of the NOTCH1 3′-UTR and CYCLIN D1 3′-UTR by hsa-miR-663b, hsa-miR-16-5p, and hsa-miR-1290, the three miRNAs of the most abundant miRNAs in CSSC-EVs. (**B**) The amount of miR-663b was significantly increased in miR-663b transfected LESCs. The expression of p63a was obviously increased and the K12 was decreased in miR-663b treated LESCs. (**C**) Representative immunofluorescence images of p63α, K12, and K14 in LESCs treated with or without miR-663b were shown. (**D**) The cascade of the Notch signaling pathway, including Notch1, NICD, and Hes1, were lower in miR-663b treated LESCs than in the controls.

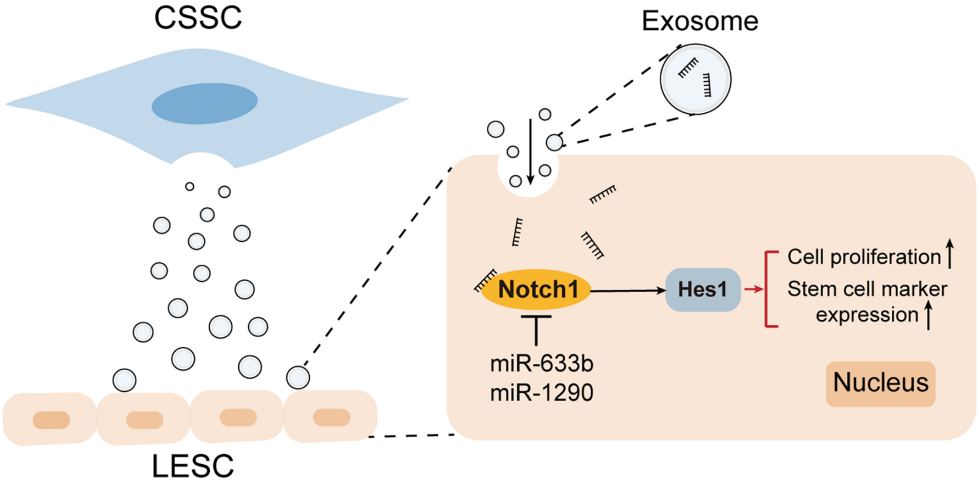

Figure 7. Schematic illustration showing that CSSC-EVs mediated the LESC phenotype by regulating the Notch1 pathway through miRNAs.

Discussion

In this study, we demonstrated that LESCs cultured in a 3D culture system that consisted of CSSCs and LESCs produced LESC outgrowths with a very homogeneous morphology and a significantly higher number of p63α^{bright} cells. Moreover, we explored the paracrine mechanism of CSSCs and especially focused on the EVs and their miRNAs in inhibiting Notch signaling expression and increasing the stemness and proliferation of LESCs. The presented data may contribute to a better understanding of the physiology of the limbal niche and open a new perspective on LESC culture and topical usage of CSSC-EVs in corneal epithelial diseases.

P63 was known to be involved in tumor suppression, morphogenesis, and master regulator of epidermal differentiation, and was the marker for LESCs. A previous study concluded that LESC grafts containing more than 3% p63α^{bright} cells led to a graft success rate of 76%. If not, only 11% of individuals have a stable ocular surface.[15] Hence, the percentage of p63α^{bright} cells is a crucial indicator for evaluating the LESC culture system. In the current research, the percentage of p63α^{bright} cells increased significantly and reached 40.5% and 41.5% in direct 3D and indirect 3D culture systems, respectively. Additionally, the required time for limbal explants to reach confluence (4.67 cm^2) in a 3D culture system was approximately 9 days (data not shown), which was much shorter than the previously reported 21 days necessary for confluence in a 2 cm^2 well.[16] Moreover, the 3D culture system mimics the spatial environment of the limbal niche, maintains the polarity of LESCs, and avoids cross-contamination with feeder cells.[17] Taken together, the results indicate that the 3D method shortens the culture time and yields more p63α^{bright} cells than the 2D culture method, which implied that the 3D method could be used in future LESC culture for limbal epithelial transplantation.

LESCs lose their stemness in the absence or with the dysregulation of the appropriate molecular signals, growth factors, and mechanical cues, which also cause transplantation failure unless the appropriate niche factors are present to maintain their stemness. Hence, comprehending how niche variables regulate LESCs at the molecular level is essential for mimicking an ex vivo environment for LESCs that preserves their phenotype in culture and after transplantation.[18] CSSCs that are located in the anterior stroma subjacent to the epithelial basement membrane are crucial limbal niche cells.[19] Numerous studies have explored the regenerative, potent immunomodulatory, and antiangiogenic properties of CSSCs,[8,20,21] which makes them attractive for clinical application. Zhu et al.[10] found that co-transplantation of LESCs and CSSCs in LSCD treatment was more effective in restoring corneal transparency than simple LESC transplantation. Li et al. demonstrated that CSSCs showed more power in preventing LSCD than bone marrow-derived mesenchymal stem cells.[22] Using a direct 3D culture method, a previous study revealed that LESCs and MSCs have direct intercellular contact.[9] However, to our knowledge, no study has compared the direct 3D method with the indirect 3D method for LESCs and CSSCs to rule out any cell-to-cell contact influences and simultaneously investigate the paracrine effect of CSSCs on LESCs. The current study demonstrated that direct 3D and indirect 3D culture systems displayed similar efficiency in promoting the stemness and proliferation of LESCs, which confirmed that CSSCs exert their effect partly through paracrine mechanisms.

Nanosized EVs have been widely reported to mediate intercellular communication in a paracrine fashion and could mimic the function of parental cells by transferring their components, such as mRNA, miRNAs, proteins, and lipids, to recipient cells.[23,24] The characteristics of bioregulatory capabilities, cell-free status, and storage for long periods make EVs a promising strategy for ex vivo culture and therapy.[25] Fai Yam et al. found that the expression of miR-29a in CSSC-EVs distinguished CSSCs with anti-scarring effects. Leszczynska et al.[26] concluded that limbal keratocyte EVs from control subjects and patients with diabetes have different efficiencies in regulating the migration and proliferation of LESCs. Ravand et al.[27] revealed that human CSSC-EVs accelerate murine corneal epithelial wound healing, but the potential mechanism has not been elucidated. The current research quantitatively compared the efficiency of CSSC-EVs in regulating the LESC phenotype, revealed the miRNA profile in CSSC-EVs, and further provided evidence that the Notch pathway was regulated by CSSC-EVs.

Notch signaling regulates the phenotype of LESCs, which has been tested by chemical molecules that block or activate the Notch pathway.[18,28–31] The miRNA sequence verified that miR-663b was the most abundant miRNA in CSSC-EVs. Previous studies on miR-663b were mostly related to cancer and suggested that miR-663b induced cell proliferation and stemness by regulating Ras/Raf signaling[32] and SMAD7.[33,34] In the current study, miRNAs in CSSC-EVs targeted *Notch1* and led to the downregulation of NICD and Hes1, and the upregulation of the important progenitor cell marker p63α, which bridged the gap of miR-633 in the field of ocular surface and the mechanism of CSSC-EVs in the limbal niche. Notably, Notch signaling has crosstalk with other pathways, such as Wnt, NF-κB, and PPARγ.[35–38] The Notch-Wnt interactions that determine the fate of epithelial cells have been demonstrated in the intestine; nevertheless, the role of the interaction is still largely unknown in the limbal niche. Moreover, NF-κB and PPARγ are the central regulators of ocular surface inflammatory diseases, such as dry eye and infectious diseases. The presented results will help us develop more therapeutic approaches by targeting the niche and its cellular components for the treatment of various corneal diseases.

A major limitation of this study is that the limbal explant was used in the study and unavoidably contained some CSSCs in the limbal tissue, because the single LESCs attached to uncoated PET membrane difficulty. It should be noticed that the CSSCs in the explant can promote the LESCs growth. Further studies with CSSCs cultured on the top and single LESC cultured on the fibrin-coated culture plate might be a better method to investigate the paracrine between niche cells and LESCs. In addition, if the limbal explant culture was needed, the explant could be removed after LESCs have migrated from the explants to reduce the potential impact of niche cells in the explant. Besides, the LESCs were administrated with CSSC-EVs on days 1, 3, and 5 in the current study. The optimal concentration and frequency of CSSC-EVs still needed to be investigated. Additionally, CSSC-EVs might have other functions in maintaining the homeostasis of the limbal niche, such as immunomodulation and regulation of blood vessel formation. Further research is needed to elucidate the physiology and confirm the therapeutic value of CSSC-EVs in corneal diseases. Finally, the LESCs cultured in the GW4869 system increased stem cell marker expression and proliferation, which implied that in addition to CSSC-EVs, other ingredients in the secretome of

Investigative Ophthalmology & Visual Science

CSSCs may have contributed to the intercellular communication between LESCs and CSSCs that still need to be explored.

Our study demonstrated that CSSC-EVs had an important role in regulating LESCs and could be used as a supplement to medium to expand the LESC population, as they retain the stemness and promote proliferation of LESCs by targeting the Notch pathway via miRNAs. Moreover, the potential characteristics of regeneration, immunoregulation and anti-neovascularization of CSSC-EVs shed light on limbal stem cell transplantation and other corneal epithelial diseases.

Acknowledgments

Supported by grants from the National Nature Science Foundation of China (Grant no. 81970765).

Disclosure: **L. Wang**, None; **X. Xu**, None; **Q. Chen**, None; **Y. Wei**, None; **Z. Wei**, None; **Z.-B. Jin**, None; **Q. Liang**, None

References

1. Schermer A, Galvin S, Sun TT. Differentiation-related expression of a major 64K corneal keratin in vivo and in culture suggests limbal location of corneal epithelial stem cells. *J Cell Biol*. 1986;103(1):49–62.
2. Deng SX, Borderie V, Chan CC, et al. Global consensus on definition, classification, diagnosis, and staging of limbal stem cell deficiency. *Cornea*. 2019;38(3):364–375.
3. Le Q, Xu J, Deng SX. The diagnosis of limbal stem cell deficiency. *Ocul Surf*. 2018;16(1):58–69.
4. Cheung AY, Sarnicola E, Denny MR, Sepsakos L, Auteri NJ, Holland EJ. Limbal stem cell deficiency: demographics and clinical characteristics of a large retrospective series at a single tertiary referral center. *Cornea*. 2021;40(12):1525–1531.
5. Ghareeb AE, Lako M, Figueiredo FC. Recent advances in stem cell therapy for limbal stem cell deficiency: a narrative review. *Ophthalmol Ther*. 2020;9(4):809–831.
6. Deng SX, Kruse F, Gomes JAP, et al. Global consensus on the management of limbal stem cell deficiency. *Cornea*. 2020;39(10):1291–1302.
7. Nakamura T, Inatomi T, Sotozono C, Koizumi N, Kinoshita S. Ocular surface reconstruction using stem cell and tissue engineering. *Progr Retin Eye Res*. 2016;51:187–207.
8. Funderburgh JL, Funderburgh ML, Du Y. Stem cells in the limbal stroma. *Ocul Surf*. 2016;14(2):113–120.
9. González S, Mei H, Nakatsu MN, Baclagon ER, Deng SX. A 3D culture system enhances the ability of human bone marrow stromal cells to support the growth of limbal stem/progenitor cells. *Stem Cell Res*. 2016;16(2):358–364.
10. Zhu L, Zhang W, Zhu J, et al. Cotransplantation of limbal epithelial and stromal cells for ocular surface reconstruction. *Ophthalmol Sci*. 2022;2(2):100148.
11. Nurković JS, Vojinović R, Dolićanin Z. Corneal stem cells as a source of regenerative cell-based therapy. *Stem Cells Int*. 2020;2020:8813447.
12. Elsharkasy OM, Nordin JZ, Hagey DW, et al. Extracellular vesicles as drug delivery systems: why and how? *Adv Drug Deliv Rev*. 2020;159:332–343.
13. Yaghoubi Y, Movassaghpour A, Zamani M, Talebi M, Mehdizadeh A, Yousefi M. Human umbilical cord mesenchymal stem cells derived-exosomes in diseases treatment. *Life Sci*. 2019;233:116733.
14. Ouyang H, Xue Y, Lin Y, et al. WNT7A and PAX6 define corneal epithelium homeostasis and pathogenesis. *Nature*. 2014;511(7509):358–361.
15. Rama P, Matuska S, Paganoni G, Spinelli A, De Luca M, Pellegrini G. Limbal stem-cell therapy and long-term corneal regeneration. *New Engl J Med*. 2010;363(2):147–155.
16. Brejchova K, Trosan P, Studeny P, et al. Characterization and comparison of human limbal explant cultures grown under defined and xeno-free conditions. *Exp Eye Res*. 2018;176:20–28.
17. Mei H, González S, Nakatsu MN, et al. A three-dimensional culture method to expand limbal stem/progenitor cells. *Tissue Eng Part C, Meth*. 2014;20(5):393–400.
18. Robertson SYT, Roberts JS, Deng SX. Regulation of limbal epithelial stem cells: importance of the niche. *Int J Mol Sci*. 2021;22(21):11975.
19. Pinnamaneni N, Funderburgh JL. Concise review: stem cells in the corneal stroma. *Stem Cells (Dayton, Ohio)*. 2012;30(6):1059–1063.
20. Veréb Z, Póliska S, Albert R, et al. Role of human corneal stroma-derived mesenchymal-like stem cells in corneal immunity and wound healing. *Sci Rep*. 2016;6:26227.
21. Al-Jaibaji O, Swioklo S, Connon CJ. Mesenchymal stromal cells for ocular surface repair. *Exp Opin Biologic Ther*. 2019;19(7):643–653.
22. Li G, Zhang Y, Cai S, et al. Human limbal niche cells are a powerful regenerative source for the prevention of limbal stem cell deficiency in a rabbit model. *Sci Rep*. 2018;8(1):6566.
23. Qiu G, Zheng G, Ge M, et al. Mesenchymal stem cell-derived extracellular vesicles affect disease outcomes via transfer of microRNAs. *Stem Cell Res Ther*. 2018;9(1):320.
24. Wang L, Wang X, Chen Q, et al. MicroRNAs of extracellular vesicles derived from mesenchymal stromal cells alleviate inflammation in dry eye disease by targeting the IRAK1/TAB2/NF-κB pathway. *Ocul Surf*. 2023;28:131–140.
25. Li N, Zhao L, Wei Y, Ea VL, Nian H, Wei R. Recent advances of exosomes in immune-mediated eye diseases. *Stem Cell Res Ther*. 2019;10(1):278.
26. Leszczynska A, Kulkarni M, Ljubimov AV, Saghizadeh M. Exosomes from normal and diabetic human corneolimbal keratocytes differentially regulate migration, proliferation and marker expression of limbal epithelial cells. *Sci Rep*. 2018;8(1):15173.
27. Yam GH, Yang T, Geary ML, et al. Human corneal stromal stem cells express anti-fibrotic microRNA-29a and 381-5p - a robust cell selection tool for stem cell therapy of corneal scarring. *J Advanced Res*. 2023;45:141–155.
28. Sartaj R, Zhang C, Wan P, et al. Characterization of slow cycling corneal limbal epithelial cells identifies putative stem cell markers. *Sci Rep*. 2017;7(1):3793.
29. Dhamodaran K, Subramani M, Krishna L, et al. Temporal regulation of notch signaling and its influence on the differentiation of ex vivo cultured limbal epithelial cells. *Curr Eye Res*. 2020;45(4):459–470.
30. González S, Uhm H, Deng SX. Notch inhibition prevents differentiation of human limbal stem/progenitor cells in vitro. *Sci Rep*. 2019;9(1):10373.
31. González S, Halabi M, Ju D, Tsai M, Deng SX. Role of Jagged1-mediated notch signaling activation in the differentiation and stratification of the human limbal epithelium. *Cells*. 2020;9(9):1945.
32. Hong S, Yan Z, Wang H, Ding L, Song Y, Bi M. miR-663b promotes colorectal cancer progression by activating Ras/Raf signaling through downregulation of TNK1. *Human Cell*. 2020;33(1):104–115.
33. Wang M, Jia M, Yuan K. MicroRNA-663b promotes cell proliferation and epithelial mesenchymal transition by directly targeting SMAD7 in nasopharyngeal carcinoma. *Exp Ther Med*. 2018;16(4):3129–3134.

Investigative Ophthalmology & Visual Science

34. Sharma B, Randhawa V, Vaiphei K, Gupta V, Dahiya D, Agnihotri N. Expression of miR-18a-5p, miR-144-3p, and miR-663b in colorectal cancer and their association with cholesterol homeostasis. *J Steroid Biochem Molec Biol*. 2021;208:105822.
35. Nakamura T, Tsuchiya K, Watanabe M. Crosstalk between Wnt and Notch signaling in intestinal epithelial cell fate decision. *J Gastroenterol*. 2007;42(9):705–710.
36. Fre S, Pallavi SK, Huyghe M, et al. Notch and Wnt signals cooperatively control cell proliferation and tumorigenesis in the intestine. *Proc Natl Acad Sci USA*. 2009;106(15):6309–6314.
37. Kay SK, Harrington HA, Shepherd S, et al. The role of the Hes1 crosstalk hub in Notch-Wnt interactions of the intestinal crypt. *PLoS Computation Biol*. 2017;13(2):e1005400.
38. Nickoloff BJ, Qin JZ, Chaturvedi V, Denning MF, Bonish B, Miele L. Jagged-1 mediated activation of notch signaling induces complete maturation of human keratinocytes through NF-kappaB and PPARgamma. *Cell Death Differ*. 2002;9(8):842–855.

Investigative Ophthalmology & Visual Science